



High-Pressure Hydrogen Sulfide from First Principles: A Strongly Anharmonic Phonon-Mediated Superconductor

Ion Errea,^{1,2} Matteo Calandra,^{3,*} Chris J. Pickard,⁴ Joseph Nelson,⁵ Richard J. Needs,⁵ Yinwei Li,⁶ Hanyu Liu,⁷ Yunwei Zhang,⁸ Yanming Ma,⁸ and Francesco Mauri³

¹*Donostia International Physics Center (DIPC), Manuel de Lardizabal Pasealekua 4, 20018 Donostia-San Sebastián, Basque Country, Spain*

²*IKERBASQUE, Basque Foundation for Science, Bilbao, Spain*

³*IMPMC, UMR CNRS 7590, Sorbonne Universités-UPMC University Paris 06, MNHN, IRD, 4 Place Jussieu, F-75005 Paris, France*

⁴*Department of Physics & Astronomy, University College London, Gower Street, London WC1E 6BT, United Kingdom*

⁵*Theory of Condensed Matter Group, Cavendish Laboratory, J.J. Thomson Avenue, Cambridge CB3 0HE, United Kingdom*

⁶*School of Physics and Electronic Engineering, Jiangsu Normal University, Xuzhou 221116, People's Republic of China*

⁷*Department of Physics and Engineering Physics, University of Saskatchewan, Saskatchewan S7N 5E2, Canada*

⁸*State Key Laboratory of Superhard Materials, Jilin University, Changchun 130012, People's Republic of China*

(Received 10 February 2015; published 16 April 2015)

We use first-principles calculations to study structural, vibrational, and superconducting properties of H₂S at pressures $P \geq 200$ GPa. The inclusion of zero-point energy leads to two different possible dissociations of H₂S, namely $3\text{H}_2\text{S} \rightarrow 2\text{H}_3\text{S} + \text{S}$ and $5\text{H}_2\text{S} \rightarrow 3\text{H}_3\text{S} + \text{HS}_2$, where both H₃S and HS₂ are metallic. For H₃S, we perform nonperturbative calculations of anharmonic effects within the self-consistent harmonic approximation and show that the harmonic approximation strongly overestimates the electron-phonon interaction ($\lambda \approx 2.64$ at 200 GPa) and T_c . Anharmonicity hardens H—S bond-stretching modes and softens H—S bond-bending modes. As a result, the electron-phonon coupling is suppressed by 30% ($\lambda \approx 1.84$ at 200 GPa). Moreover, while at the harmonic level T_c decreases with increasing pressure, the inclusion of anharmonicity leads to a T_c that is almost independent of pressure. High-pressure hydrogen sulfide is a strongly anharmonic superconductor.

DOI: [10.1103/PhysRevLett.114.157004](https://doi.org/10.1103/PhysRevLett.114.157004)

PACS numbers: 74.62.Fj, 63.20.dk, 71.15.Mb, 74.25.Jb

Cuprates [1] have for many years held the world record for the highest superconducting critical temperature ($T_c = 133$ K) [2]. However, despite almost 30 years of intensive research, the physical mechanism responsible for such a high T_c is still elusive, although the general consensus is that it is highly nonconventional. The measurements by Drozdov *et al.* [3] which suggest a 190 K superconducting phase in hydrogen sulfide under high pressure (200 GPa), could break the cuprates record, if confirmed.

The claim that hydrogen at high pressure could be superconducting is not new [4] and it was recently supported by first-principles calculations based on the harmonic approximation applied to dense hydrogen [5–8] and several hydrides [9–15]. More recently, two theoretical papers predicted the occurrence of high- T_c superconductivity in high-pressure sulfur hydrides [16,17]. However, as shown in Refs. [18,19], anharmonicity can be crucial in these systems. For example, in PdH, the electron-phonon coupling λ parameter is found to be 1.55 at the harmonic level, while a proper inclusion of anharmonic effects leads to $\lambda = 0.40$ [18], in better agreement with experiments. Thus, in hydrogen-based compounds, the phonon spectra are strongly affected by anharmonic effects.

Given the sensitivity of superconductivity to the physical and electronic structures, it is extremely important to

identify the correct crystal structures (see, for example, the early discussion of superconductivity in silane in Ref. [15], and one of the first applications of first-principles structure prediction in Ref. [20]). Several first-principles calculations [16,17,21–23] suggested that decomposition of the H₂S sample occurs within the diamond-anvil cell at high pressures. The high- T_c superconducting material is therefore very unlikely to be H₂S, while H₃S is the obvious candidate for the H-rich decomposition product.

Here we study the structural, vibrational, and superconducting properties of H₂S above 200 GPa, where the highest T_c occurs. We show that the inclusion of zero-point motion in the convex hull at 200 and 250 GPa stabilizes two metallic structures, H₃S and HS₂. Finally, we show that, contrary to suggestions in previous work [16,21], the harmonic approximation does not explain the measured T_c in H₃S, and the inclusion of anharmonic effects is crucial.

As decomposition of H₂S has been demonstrated in the experiments of Ref. [3], it is crucial to develop an understanding of the different H-S compounds that might be stable in the pressure range of interest. We therefore perform a search over 44 H:S stoichiometries, determining the stoichiometries at which stable structures exist, and the associated crystal structures. These searches were performed with the *ab initio* random structure searching

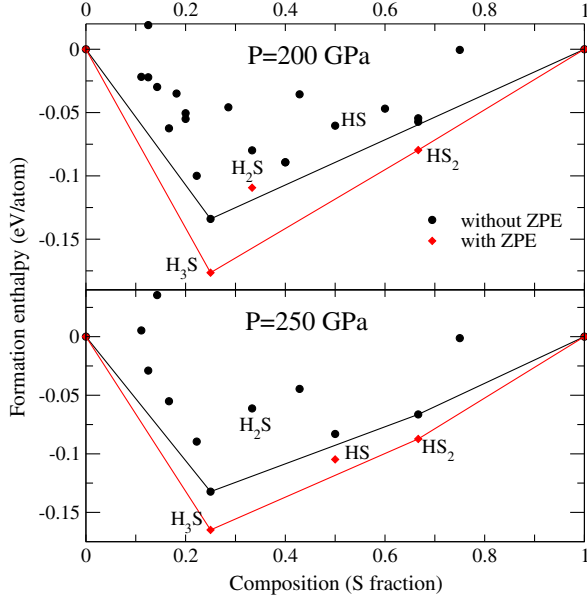


FIG. 1 (color online). Results of structure searching at 200 and 250 GPa. Convex hulls are shown as continuous lines, with and without the inclusion of zero-point energy (ZPE).

(AIRSS) method [20,24] and the CASTEP code [25], and the CALYPSO particle-swarm optimization method [26,27] and the VASP code [28,29]. More information about the searches is provided in the Supplemental Material [30].

The results of the structure searching are shown in Fig. 1. At 200 GPa, without zero-point energy (ZPE), the only energetically allowed decomposition is $3\text{H}_2\text{S} \rightarrow 2\text{H}_3\text{S} + \text{S}$, in agreement with previous calculations [16,21,22,34]. H_3S crystallizes in the space group $Im\bar{3}m$, as shown in Ref. [16]. When ZPE is included, a second decomposition becomes possible at 200 GPa, namely $5\text{H}_2\text{S} \rightarrow 3\text{H}_3\text{S} + \text{HS}_2$, where HS_2 crystallizes in a structure of space group $C2/c$ with 12 atoms/cell. At 250 GPa and above, the latter decomposition is allowed even without ZPE, and the $C2/c$ HS_2 structure undergoes a phase transition to a more stable $C2/m$ structure with 6 atoms/cell. Each of the HS_2 structures is metallic. Finally, at 300 GPa, a metallic HS phase with $C2/m$ space group becomes stable [30]. Detailed information on the crystal structures is provided in the Supplemental Material [30].

Having determined the most stable crystal structures at high pressure, we turn to the study of vibrational properties [35,36]. As summarized in Table I, the superconducting T_c values obtained within the harmonic approximation for the $C2/c$ HS_2 , $C2/m$ HS_2 , and $C2/m$ HS phases are in the range of 15 to 35 K (see Supplemental Material [30] for phonon spectra and details of the calculations), far from the observed extraordinary values. The measured T_c 's could not have occurred in any of these phases. Thus, we focus on the $Im\bar{3}m$ H_3S structure. In this structure, each H atom is twofold coordinated and has 6 neighbors, 2 of which are S atoms while the other 4 are H atoms. The H vibrations can

TABLE I. Calculated λ , ω_{\log} , and T_c values in the harmonic approximation for $C2/c$ HS_2 , $C2/m$ HS_2 , and $C2/m$ HS . T_c is estimated using the McMillan equation.

Phase	P (GPa)	λ	ω_{\log} (meV)	$T_c^{\mu^* = 0.10}$ (K)	$T_c^{\mu^* = 0.16}$ (K)
$C2/c$ HS_2	200	0.86	56.7	35.3	23.4
$C2/m$ HS_2	250	0.75	53.8	25.1	14.9
$C2/m$ HS	300	0.78	74.3	38.0	23.4

then be decomposed into H–S bond-stretching modes (H_{\parallel}), in which an H atom moves toward one of the two S atoms, and bond-bending modes (H_{\perp}), in which one H atom moves in the direction perpendicular to the H–S bond (see

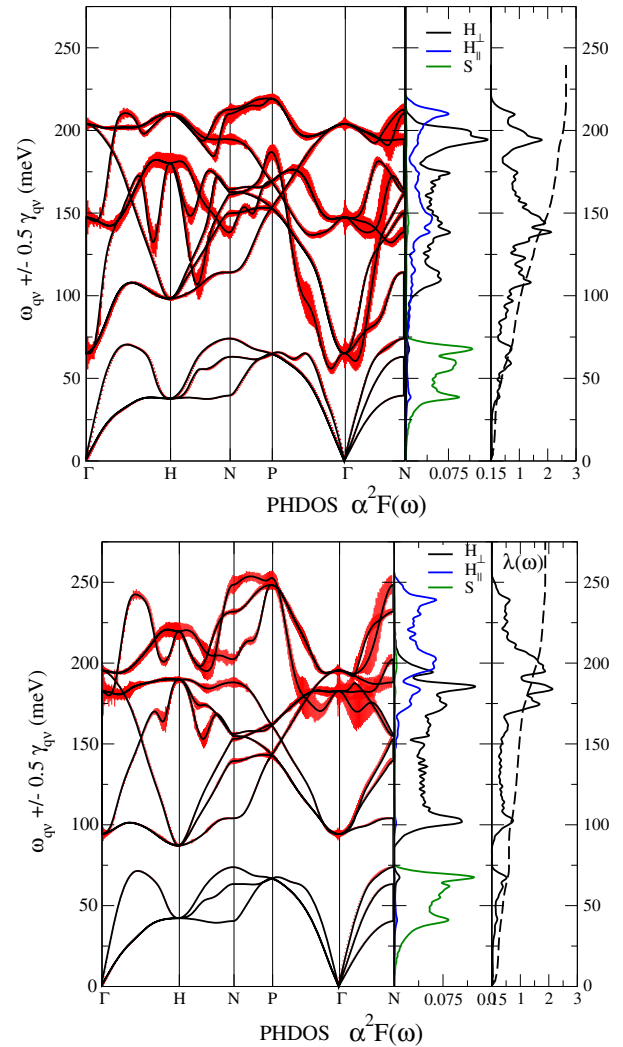


FIG. 2 (color online). Phonon dispersion, phonon density of states projected onto selected atoms and directions, and the Eliashberg function of H_3S in the harmonic approximation (top) and with the inclusion of anharmonic effects (bottom) for H_3S at 200 GPa. H_{\perp} and H_{\parallel} label displacements of an H atom in the directions perpendicular or parallel to a H–S bond. The magnitude of the phonon linewidth is indicated by the size of the red error bars.

Fig. 1 in the Supplemental Material [30]). The harmonic phonon spectrum of H₃S at 200 GPa [39] is shown in Fig. 2 and overall shows a clear separation into H modes at high energy and S modes below 75 meV. To gain more insight, we use Wannier interpolation [40,41] of the electron-phonon matrix elements and evaluate the electron-phonon contribution to the phonon linewidth as [42]

$$\gamma_{\mathbf{q}\nu} = \frac{4\pi\omega_{\mathbf{q}\nu}}{N_k} \sum_{\mathbf{k},n,m} |g'_{nm}(\mathbf{k}, \mathbf{k} + \mathbf{q})|^2 \delta(\epsilon_{\mathbf{k}n}) \delta(\epsilon_{\mathbf{k}+\mathbf{q}m}). \quad (1)$$

Here, $\omega_{\mathbf{q}\nu}$ are the phonon frequencies, N_k the number of electron-momentum points in the grid, $g'_{nm}(\mathbf{k}, \mathbf{k} + \mathbf{q}) = \langle \mathbf{k}n | \delta V_{\text{KS}} / \delta u_{\mathbf{q}\nu} | \mathbf{k} + \mathbf{q}m \rangle$ is the electron-phonon matrix element, V_{KS} is the Kohn-Sham potential, and $u_{\mathbf{q}\nu}$ is a phonon displacement. The Kohn-Sham energy and eigenfunctions are labeled $\epsilon_{\mathbf{k}n}$ and $|\mathbf{k}n\rangle$. The electron-phonon coupling at a given phonon-momentum \mathbf{q} for a phonon mode ν can be obtained [42] from the phonon linewidth as $\lambda_{\mathbf{q}\nu} = \{\gamma_{\mathbf{q}\nu} / [2\pi\omega_{\mathbf{q}\nu}^2 N(0)]\}$.

As shown in Fig. 2, at the harmonic level, the phonon linewidths of the H vibrations are fairly uniform throughout the spectrum. The contribution of each mode to the average electron-phonon interaction, $\lambda = \sum_{\nu\mathbf{q}} \lambda_{\mathbf{q}\nu} / N_q$, can be obtained from the isotropic Eliashberg function,

$$\alpha^2 F(\omega) = \frac{1}{2N_q} \sum_{\mathbf{q}\nu} \lambda_{\mathbf{q}\nu} \omega_{\mathbf{q}\nu} \delta(\omega - \omega_{\mathbf{q}\nu}), \quad (2)$$

where N_q is the number of phonon-momentum points in the grid. $\lambda(\omega) = 2 \int_0^\omega [\alpha^2 F(\omega') / \omega'] d\omega'$ and then $\lambda = \lambda(\infty)$. We find $\lambda = 2.64$ (see Table II), which is larger than that obtained in Refs. [16,21] with a much coarser sampling of the BZ, but consistent with the result in Ref. [22]. This huge value of λ comprises substantial contributions from many H vibrational modes. The situation is therefore very different from MgB₂ in which a single mode dominates λ .

Given the low mass of H and the consequent large phonon displacements, we investigate the occurrence of anharmonic effects using the stochastic self-consistent harmonic approximation (SSCHA) developed by some of us [18,19,43]. As shown in Fig. 2 (bottom), the anharmonic correction leads to nontrivial changes in the

harmonic spectrum. While it is very clear that all H bond-stretching modes are hardened, the effect on H bond-bending modes is less straightforward. By computing the average phonon frequency as of H_{||} and of H_⊥ modes, we find that $\bar{\omega}_{||}^{\text{har}} \approx 158.1$ meV and $\bar{\omega}_{||}^{\text{anh}} \approx 203.3$ meV, while for bond-bending modes $\bar{\omega}_{\perp}^{\text{har}} \approx 157.0$ meV and $\bar{\omega}_{\perp}^{\text{anh}} \approx 147.9$ meV. Thus bond-stretching modes are hardened, while bond-bending modes are softened.

It is important to remark that the large and most dispersive mode along $\Gamma\Gamma$ is strongly hardened at the anharmonic level and undergoes a nontrivial change in polarization, as can be seen from the large effect of anharmonicity on the phonon linewidth $\gamma_{\mathbf{q}\nu}$ in Fig. 2. It is worthwhile recalling that the phonon linewidth depends on the phonon eigenvector but not on the phonon energy. This effect demonstrates the need to calculate not only the phonon frequencies at the anharmonic level, but also the phonon polarizations.

The anharmonic electron-phonon interaction is $\lambda = 1.84$, which is 30% smaller than the harmonic result. This reduction is mostly explained by the hardening of the H_{||} modes. In contrast to the harmonic case, which shows uniform coupling over all modes, the anharmonic Eliashberg function has two main peaks, a broad peak in the 40–75 meV region, and a second one in the 175–200 meV region. Their contributions to λ are 0.59 and 0.77, respectively, accounting for $\approx 73\%$ of the total λ . We note, however, that the logarithmic average of the phonon frequencies ω_{log} is only weakly enhanced by anharmonicity (see Table II).

The superconducting critical temperature can be obtained either from the McMillan equation or the isotropic Migdal-Eliashberg approach. However, it is well known [44] that the use of the McMillan equation for such values of λ leads to a substantial underestimation of T_c . We solved the isotropic Eliashberg equations (see the Supplemental Material [30]) and found, contrary to claims in previous publications [16,21], that calculations based on the harmonic phonon spectrum do not explain the measured T_c as, even using large values of μ^* [45,46], T_c is substantially overestimated (i.e., $T_c = 250$ K for $\mu^* = 0.16$ [30]). When the anharmonic phonon spectrum and electron-phonon coupling are used, the Migdal-Eliashberg equations account for the experimental T_c when the value $\mu^* = 0.16$

TABLE II. Electron-phonon interaction and logarithmic averages of phonon frequencies, with and without anharmonic effects. The T_c 's are calculated using the isotropic Migdal-Eliashberg equations (T_c^{ME}). A value of $\mu^* = 0.16$ is used. Data for T_c calculated with the McMillan equation are provided in the Supplemental Material [30]. Frequencies are in meV and T_c 's are in K.

Compound	λ^{har}	$\omega_{\text{log}}^{\text{har}}$	λ^{anh}	$\omega_{\text{log}}^{\text{anh}}$	$T_c^{\text{ME,har}}$	$T_c^{\text{ME,anh}}$	T_c (expt.)
H ₃ S (200 GPa)	2.64	90.4	1.84	92.86	250	194.0	190
H ₃ S (250 GPa)	1.96	109.1	1.71	101.3	226	190	
D ₃ S (200 GPa)	2.64	68.5	1.87	73.3	183	152.0	90

is used, as shown in Table II. The superconducting gap at zero temperature is $\Delta \approx 36.5$ meV. By using the smaller value of $\mu^* = 0.1$, we obtain $T_c = 222$ K and $\Delta \approx 43$ meV.

Interestingly, the large anharmonic effects lead to very different variations in T_c with pressure. By performing the harmonic electron-phonon calculation for the $Im\bar{3}m$ structure at 250 GPa and using the Migdal-Eliashberg equations with $\mu^* = 0.16$ we found $T_c = 226$ K, decreasing with increasing pressure. However, at the anharmonic level, we find $T_c = 190$ K, essentially independent of pressure in the region 200–250 GPa.

Finally, we consider the extent to which the occurrence of large anharmonic effects can explain the isotope shift in D_2S . At 164 GPa, $T_c(D_2S) = 90$ K, leading to an isotope coefficient $\alpha \approx 1.07$, which is substantially enhanced from the canonical BCS value of $\alpha \approx 0.5$. Assuming a similar decomposition of D_2S into D_3S and S at high pressures, we calculate the anharmonic phonon spectrum (see the Supplemental Material [30]) and electron-phonon coupling in D_3S at 200 GPa. We find at the anharmonic level that the electron-phonon coupling is essentially unaffected, while ω_{\log} is softened from 92.9 meV to 73.3 meV, leading to an isotope coefficient of $\alpha = 0.35$, which is strongly reduced from the BCS value. Thus, contrary to the claim made in Ref. [47], anharmonicity reduces α . As long as the same crystal structure for H_3S and D_3S is considered, as predicted by our calculation, the theoretical isotope coefficient remains inconsistent with the value of $\alpha \approx 1.07$ found in experiments. This disagreement could be reconciled if in experiment kinetics stabilize different structures for hydrides and deuterides at a given pressure. More experimental data are necessary to clarify this issue.

We have studied the structural, vibrational, and superconducting properties of high-pressure H_3S . We have included zero-point motion when comparing the stabilities of different H-S phases, which has been neglected in other publications so far. This is important because zero-point motion stabilizes a new phase at $P \geq 200$ GPa. In particular, we found that decomposition of HS_2 into metallic phases can occur following two main paths, namely $3H_2S \rightarrow 2H_3S + S$ and $5H_2S \rightarrow 3H_3S + HS_2$. We have performed a detailed study of the vibrational properties of high-pressure H_3S and D_3S , finding that the phonon spectra are strongly affected by anharmonic effects. Anharmonicity hardens H–S bond-stretching modes and softens H–S bond-bending modes. Moreover, anharmonicity leads to a reduction in the electron-phonon coupling by $\approx 30\%$ and to an approximately constant T_c in the range 200–250 GPa. Our work demonstrates that the superconducting properties of high-pressure H_3S can only be properly described by including both nuclear quantum effects and anharmonicity.

We acknowledge discussions with I. I. Mazin and support from the Agence Nationale de la Recherche, Grant

No. ANR-13-IS10-0003-01. Computer facilities were provided by PRACE, CINES, CCRT, and IDRIS. I. E. acknowledges financial support from the Department of Education, Language Policy, and Culture of the Basque Government (Grant No. BFI-2011-65) and the Spanish Ministry of Economy and Competitiveness (FIS2013-48286-C2-2-P). C. J. P. and R. J. N. thank EPSRC (UK) for financial support. J. R. N. acknowledges financial support from the Cambridge Commonwealth Trust. Y. Li thanks the National Natural Science Foundation of China for support under Grants No. 11204111 and No. 11404148. Y. Zhang and Y. Ma thank the Natural Science Foundation of China for support under Grant No. 11274136 and the 2012 Changjiang Scholars Program of China.

*matteo.calandra@upmc.fr

- [1] J. G. Bednorz and K. A. Mueller, *Z. Phys. B* **64**, 189 (1986).
- [2] A. Schilling, M. Cantoni, J. D. Guo, and H. R. Ott, *Nature (London)* **363**, 56 (1993).
- [3] A. P. Drozdov, M. I. Erements, and I. A. Troyan, arXiv:1412.0460.
- [4] N. W. Ashcroft, *Phys. Rev. Lett.* **21**, 1748 (1968).
- [5] L. Zhang, Y. Niu, Q. Li, T. Cui, Y. Wang, Y. Ma, Z. He, and G. Zou, *Solid State Commun.* **141**, 610 (2007).
- [6] P. Cudazzo, G. Profeta, A. Sanna, A. Floris, A. Continenza, S. Massidda, and E. K. U. Gross, *Phys. Rev. Lett.* **100**, 257001 (2008).
- [7] P. Cudazzo, G. Profeta, A. Sanna, A. Floris, A. Continenza, S. Massidda, and E. K. U. Gross, *Phys. Rev. B* **81**, 134505 (2010).
- [8] P. Cudazzo, G. Profeta, A. Sanna, A. Floris, A. Continenza, S. Massidda, and E. K. U. Gross, *Phys. Rev. B* **81**, 134506 (2010).
- [9] D. Y. Kim, R. H. Scheicher, C. J. Pickard, R. J. Needs, and R. Ahuja, *Phys. Rev. Lett.* **107**, 117002 (2011).
- [10] T. Scheler, O. Degtyareva, M. Marques, C. L. Guillaume, J. E. Proctor, S. Evans, and E. Gregoryanz, *Phys. Rev. B* **83**, 214106 (2011).
- [11] X.-F. Zhou, A. R. Oganov, X. Dong, L. Zhang, Y. Tian, and H.-T. Wang, *Phys. Rev. B* **84**, 054543 (2011).
- [12] D. Y. Kim, R. H. Scheicher, H.-k. Mao, T. W. Kang, and R. Ahuja, *Proc. Natl. Acad. Sci. U.S.A.* **107**, 2793 (2010).
- [13] G. Gao, A. R. Oganov, P. Li, Z. Li, H. Wang, T. Cui, Y. Ma, A. Bergara, A. O. Lyakhov, T. Iitaka, and G. Zou, *Proc. Natl. Acad. Sci. U.S.A.* **107**, 1317 (2010).
- [14] G. Gao, A. R. Oganov, A. Bergara, M. Martinez-Canales, T. Cui, T. Iitaka, Y. Ma, and G. Zou, *Phys. Rev. Lett.* **101**, 107002 (2008).
- [15] J. Feng, W. Grochala, T. Jaron, R. Hoffmann, A. Bergara, and N. W. Ashcroft, *Phys. Rev. Lett.* **96**, 017006 (2006).
- [16] D. Duan, Y. Liu, F. Tian, D. Li, X.-a. Huang, Z. Zhao, H. Yu, B. Liu, W. Tian, and T. Cui, *Sci. Rep.* **4**, 6968 (2014).
- [17] Y. Li, J. Hao, H. Liu, Y. Li, and Y. Ma, *J. Chem. Phys.* **140**, 174712 (2014).
- [18] I. Errea, M. Calandra, and F. Mauri, *Phys. Rev. Lett.* **111**, 177002 (2013).

- [19] I. Errea, M. Calandra, and F. Mauri, *Phys. Rev. B* **89**, 064302 (2014).
- [20] C. J. Pickard and R. J. Needs, *Phys. Rev. Lett.* **97**, 045504 (2006).
- [21] J. A. Flores-Livas, A. Sanna, and E. K. U. Gross, [arXiv:1501.06336](https://arxiv.org/abs/1501.06336).
- [22] R. Akashi, M. Kawamura, S. Tsuneyuki, Y. Nomura, and R. Arita, [arXiv:1502.00936](https://arxiv.org/abs/1502.00936).
- [23] D. Duan, X. Huang, F. Tian, D. Li, Hongyu, Yu, Y. Liu, Y. Ma, B. Liu, and T. Cui, [arXiv:1501.01784](https://arxiv.org/abs/1501.01784).
- [24] C. J. Pickard and R. J. Needs, *J. Phys. Condens. Matter* **23**, 053201 (2011).
- [25] S. J. Clark, M. D. Segall, C. J. Pickard, P. J. Hasnip, M. I. J. Probert, K. Refson, and M. C. Payne, *Z. Kristallogr.* **220**, 567 (2005).
- [26] Y. Wang, J. Lv, L. Zhu, and Y. Ma, *Comput. Phys. Commun.* **183**, 2063 (2012).
- [27] Y. Wang, J. Lv, L. Zhu, and Y. Ma, *Phys. Rev. B* **82**, 094116 (2010).
- [28] G. Kresse and J. Furthmüller, *Comput. Mater. Sci.* **6**, 15 (1996).
- [29] G. Kresse and J. Furthmüller, *Phys. Rev. B* **54**, 11169 (1996).
- [30] See Supplemental Material at <http://link.aps.org/supplemental/10.1103/PhysRevLett.114.157004> for convex hull of H_xS_y at 300 GPa, the effect of the zero-point energy on the convex hull at 200 GPa, crystal structures, electronic structure of H_3S , vibrational properties of D_3S at 200 GPa and H_3S at 250 GPa, solution of Migdal-Eliashberg equations, the effects of the vibrational zero-point energy on pressure, electronic and vibrational properties of HS_2 and HS phases. Supplemental Material includes Refs. [31–33].
- [31] A. Togo, F. Oba, and I. Tanaka, *Phys. Rev. B* **78**, 134106 (2008).
- [32] C. J. Pickard and R. J. Needs, *Nat. Phys.* **3**, 473 (2007).
- [33] O. Degtyareva, E. Gregoryanz, M. Somayazulu, H.-k. Mao, and R. J. Hemley, *Phys. Rev. B* **71**, 214104 (2005).
- [34] N. Bernstein, C. S. Hellberg, M. D. Johannes, I. I. Mazin, and M. J. Mehl, *Phys. Rev. B* **91**, 060511 (2015).
- [35] P. Giannozzi *et al.*, *J. Phys. Condens. Matter* **21**, 395502 (2009).
- [36] Our superconductivity results were obtained from first-principles DFT linear-response calculations as implemented in the QUANTUM-ESPRESSO [35] package. We used ultrasoft [37] pseudopotentials, a generalized gradient approximation [38], a plane-wave cutoff energy of 60 Ry on the kinetic energy and 600 Ry on the charge density. The charge density and dynamical matrices were calculated using a 32^3 Monkhorst-Pack shifted electron-momentum grid and a Hermitian-Gaussian smearing of 0.03 Ry. The average electron-phonon coupling was obtained using Wannier interpolation [40]. We used a 32^3 electron-momentum grid randomly shifted from the origin and a 32^3 Monkhorst-Pack shifted phonon-momentum grid with a smearing of 0.03 eV. The phonon linewidth at a given phonon momentum was calculated using a $50 \times 50 \times 50$ electron-momentum mesh (randomly shifted from the origin).
- [37] D. Vanderbilt, *Phys. Rev. B* **41**, 7892 (1990).
- [38] J. P. Perdew, K. Burke, and M. Ernzerhof, *Phys. Rev. Lett.* **77**, 3865 (1996).
- [39] The pressure computed here is without inclusion of ZPE. Neglecting ZPE underestimates the pressure of ≈ 12 GPa for H_3S and 6 GPa for D_3S for a volume of 89.9822 (a.u.)³. See the Supplemental Material [30] for more details.
- [40] M. Calandra, G. Profeta, and F. Mauri, *Phys. Rev. B* **82**, 165111 (2010).
- [41] F. Giustino, J. R. Yates, I. Souza, M. L. Cohen, and G. Louie, *Phys. Rev. Lett.* **98**, 047005 (2007).
- [42] P. B. Allen, *Phys. Rev. B* **6**, 2577 (1972); P. B. Allen and R. Silbergliitt, *Phys. Rev. B* **9**, 4733 (1974).
- [43] The SSCHA calculations were performed using a $3 \times 3 \times 3$ supercell for both H_3S and D_3S at 0 K, yielding dynamical matrices on a commensurate $3 \times 3 \times 3$ q -point grid. An additional calculation at 200 K confirmed that temperatures within the range of the predicted superconductivity do not affect the phonon spectra. The difference between the harmonic and anharmonic dynamical matrices in the $3 \times 3 \times 3$ phonon-momentum grid was interpolated to a $6 \times 6 \times 6$ grid. Adding the harmonic matrices to the result, the anharmonic dynamical matrices were obtained in a $6 \times 6 \times 6$ grid. These dynamical matrices were used for the anharmonic electron-phonon coupling calculation.
- [44] P. B. Allen and R. C. Dynes, *Phys. Rev. B* **12**, 905 (1975).
- [45] P. Morel and P. W. Anderson, *Phys. Rev.* **125**, 1263 (1962).
- [46] N. N. Bogoliubov, V. V. Tolmachev, and D. V. Shirkov, *A New Method in the Theory of Superconductivity* (Consultants Bureau, New York, 1959).
- [47] D. A. Papaconstantopoulos, B. M. Klein, M. J. Mehl, and W. E. Pickett, [arXiv:1501.03950v1](https://arxiv.org/abs/1501.03950v1).